A CONTRIBUTION TO THE LMFBR FUEL PIN BEHAVIOUR DURING TRANSIENT OVERPOWER CONDITIONS

B. KUCZERA

Institut für Reaktorentwicklung, Kernforschungszentrum Karlsruhe, D-7500 Karlsruhe, Germany

SUMMARY

The long-time behaviour of the fuel pins under steady state reactor conditions has been studied extensively. However, with respect to the safety analysis there exists a particular interest in the short-time behaviour of a LMFBR fuel pin during an overpower transient, and its state at the time of cladding failure.

The study presented deals with the behaviour of unirradiated fuel pins during a power excursion (reactor period = 17 msec). The pin type A (X_{max} = 420 W/cm, gap size Δs = 0.07 mm, fuel porosity $P_0 = 0.07$) will be used as a reference pin; it is similar to the fuel pin of the SNR-300. The pin type B has a smaller gap size ($\Delta s = 0.05$ mm), whereas pin type C has a larger porosity ($P_0 = 0.12$). The numerical analysis was performed with the computer code BREDA (ref. KFK-1729).

The new aspect of this study is the investigation of the influence of fuel rod design parameters on the short-time behaviour of fuel pins during the pre-disassembly phase of a hypothetical accident. The most significant results are as follows:

(1) The steady state temperature of the pin type B (average temperature of the fuel T_{Bm} = 1495°C) evidently is below the reference pin (T_{Bm} = 1640°C). This is due to the better heat transfer in the gap (fuel/clad).
The larger porosity of the pin type C decreases the heat conduction of the fuel, resulting in a higher temperature level (T_{Bm} = 1715°C). Initially the temperature T_{Bm} increases parablelike according to the energy released, but the temperature-gradient in time decreases as soon as fuel melting starts (time sequence of incipient melting: pin type C, A, B; amount of molten fuel at $t = 0.25$ sec: 0.46, 0.39, 0.29).

(2) Although the thermal expansion coefficient of the fuel is less than that of the clad the pellet expansion exceeds that of the clad. This is due to the higher temperature and temperature rate in the fuel. The increase of the fuel expansion due to volume changes on melting is smallest for the pin type C; this is caused by the higher initial porosity. As a consequence the gap will be closed rather late (time sequence: B, A, C). The mechanical fuel-clad interaction yields circumferential plastic strains, which are given by $B = 4.2\%$, $A = 3.7\%$, $C = 2.4\%$ at time $t = 0.35$ sec.

(3) Assuming failure at 3% plastic strain in the clad, both types A and B will burst within the range of time considered. The energy release at a subsequent fuel-coolant interaction (FCI) will depend, beside other parameters, on the amount of molten fuel (V_L) by the time of failure (t_V). (A: $t_V = 0.33$ sec, $V_L = 0.77$. B: $t_V = 0.31$ sec, $V_L = 0.69$). Thus, on the given assumptions, the damage potential of the FCI appears to be less for the pin type B than for the type A, since less molten fuel is present. Furthermore, with regard to the neutron kinetics, the B-type pin provides larger reserves for nuclear shutdown as a result of the Doppler-broadening. This is due to the greater difference between the steady state fuel-temperature and its melting point.

In the model theory describing the fuel pin behaviour two development trends are being pursued. Studies of the long-time behaviour supply information about changes of the fuel and the cladding tube under steady-state operating conditions and loads respectively, undergoing cyclic changes both of which depend largely on the burnup condition of the fuel pin. A different aspect can be derived from safety considerations of Liquid Metal Fast Breeder Reactors (LMFBR) analyzing the reactor behaviour during power excursions. Since these events occur in the range of milliseconds to seconds, we are interested in the short-time behaviour of a fuel pin under transient reactor conditions and its feedback on neutron physics and thermodynamics of the core. Both concepts supplement each other, resulting in better understanding of fuel pin behaviour in the spectrum of possible reactor conditions.

This paper is concerned with a parameter study analyzing the fuel pin behaviour during a hypothetical reactivity accident. Especially the influence of fuel porosity and the width of the gap (between the fuel and the cladding) upon transient fuel pin deformation and the fuel pin condition at the time of pin burst are investigated. First of all, some remarks should be made about the BREDA computer model [1, 2] used in these studies. In this model the uncoupled, quasi-steady state thermoelastic theory is assumed to apply. "Uncoupled" in this case means that the non-steady state heat conduction problem of the fuel pin is solved independently; "quasi-steady state" indicates that no forces of inertia are being considered during the process of deformation. BREDA was linked with the thermodynamic part of RADYVAR Code [3, 4], which gives the transient temperature field for the stress analysis at any point in time, while BREDA afterwards supplies the modified fuel pin geometry.

The other assumptions made are these: rotational symmetry, cross-sections remaining plane, small changes of geometry due to strain, axially constant temperature profile in a sub-zone. In this case, the well known equations of the linear theory of elasticity apply to an axial segment of the fuel pin. They are derived in a cylindrical coordinate system (r, φ, z) and using the well known notation (cf. Figure 2) take the form shown in Fig. 1.

In Fig. 1 the general solution $u(r)$ and $w(z)$ of the system of differential equations for the fuel cylinder has been indicated. With respect to the boundary conditions to be established, which are used to determine the integration constants, distinctions must be made between various cases which are guided by the previous load history and the present load condition of the fuel pin.

The solid fuel is regarded as a material with elastic properties. This also applies to the cladding tube up to the yield point of the material. Subsequently, it is assumed that the thin walled tube changes into a membrane stress condition as a consequence of the pressure stress and is able to undergo ideal plastic deformation.

Fuel pin failure occurs if the cladding tube, the so-called first barrier preventing an uncontrolled release of radioactivity, is destroyed. The causes are either induced from the outside or may be generated within the fuel pin itself. If sodium boiling occurs during an incident, this may cause the cladding to melt down after an interruption of heat removal as a consequence of dry out of sodium. On the other hand, there may be melt down of the cladding if most of the fuel has molten during the excursion. In this case, the steep temperature gradient in the gap produces the relatively high rate of heating in the cladding. The third cause of failure is excessive mechanical stress generated mainly by differential expansion in the fuel and the cladding, respectively, and resulting in plastic deformation of the cladding tube.

If a failure criterion is derived from plastic deformation of the cladding, restrictions implied by the model must be mentioned once more. It is not possible to derive the failure threshold value of the degree of plastic deformation from the model only. Since the material is assumed to behave ideally, a burst criterion fitting the model must be quantatively derived from the respective experiments. This is possible, if the time of bursting is determined experimentally, for instance, by a definable pressure pulse. The degree of plastic deformation generated at this time and determined by calculation subsequent to the experiment may then be regarded as a failure criterion equivalent to the model. So much for the computer model.

In the parameter study the power excursion was simulated by the time function of the pin power $\chi = \chi_0$ (1+100 t), feedback of reactivity on the power excursion being disregarded. The model pin resembles a fuel pin of the SNR 300 [5]. As a consequence of the modifications made, specific effects and failure tendencies should become more marked. Figure 3 is a summary of a most important input data used in the calculations. As against the reference pin "a" (gap width Δs = 0.07 mm, fuel porosity p = 0.07), pin "b" is distinguished by the smaller gap width (Δs = 0.05 mm), pin "c" by the greater porosity (p = 0.12).

In Figure 4, the temperature versus-time curve has been plotted in the fifth axial fuel pin zone as a result of the calculation for the power excursion at hand. After 0.35 sec sodium begins to boil in the eighth zone located above the fifth zone, which indicates the upper limit of the period of time considered. Corresponding to the linear time function, the power of the pin has increased by a factor of 36 within this period of time. Initially, the increase in the average fuel temperature T_{Bm} is parabolic corresponding to the power integral, and flattens off as soon as the fuel begins to melt. Qualitatively it was found that pin "c", as was to be expected, with its larger fuel porosity generates a higher temperature profile because of the lower thermal conductivity, the peak of which profile reaches the melting area much sooner. The reverse tendency is shown in pin "b" with the smaller gap width, where better heat removal from the fuel results in a generally lower temperature curve. In that case the range of heating to the melting isotherms is larger and partial melting of the fuel will occur at a later date.

The temperatures of the cladding tube must be regarded in close connection with the coolant temperatures. The differences in time are within plotting accuracy and will not be discussed in more detail.

Figure 5 shows the resultant load phenomena, such as the fraction of molten fuel and the deformation of the fuel pin, as a function of time. The similar types of melting curve found in these three cases may be due to the parabolic original temperature distribution in the fuel cross-section. Accordingly, melting does not occur simultaneously in several areas of the fuel, but the melting radius extends continuously into the boundary zones. However, the molten fractions (v_L) differ, e. g., at the time t = 0.25 sec with pin "b" with the smaller gap width $v_L = 0.29$, which is clearly below $v_L = 0.39$ of the reference pin "a". In pin "c" with the higher porosity, the molten fraction $v_L = 0.46$ is the highest because of the high steady-state temperature level.

In Figure 5, the deformation of the fuel pin is described by the time-dependent change of the radii R_2, R_3 and R_4 of the fuel pin and the degree of plastic deformation of the cladding $\epsilon_{R4} = 100 \cdot \left[R_4(t) - R_4(t=0)\right]/R_4(t=0)$. With increasing heat source density the fuel pin continues to expand. Most of this expansion is due to an expansion of the pellet because the lower thermal expansion coefficient, compared with steel, is overcompensated by the much higher rate of heating. The expansion of the fuel is enhanced by the increase in volume associated with melting. As a consequence of the reduction of gap width this brings about, the heat transfer between the fuel and the cladding is increased. In the thermodynamic model, this is described by the relation $\alpha = c/\left[R_4(t) - R_3(t)\right]$ for $\alpha \leq 2$ W/cm² °C. This influences the shape of the curve of the fuel surface temperatures T_{Bn}, which is indicated by a point of inflection, especially with pins "a" and "c". In the time of increased fuel expansion between t = 0.155 .... 0.185 sec the α-value changes from 1.44 to 2.00 W/cm² °C and is then kept constant at the last value. This corresponds to a rate of change $\Delta\alpha/\Delta t$ improving the heat transfer which is more than twice as high as that encountered in the previous time interval t = 0.125 .... 0.155 sec. When $\alpha_{max} = 2$ W/cm² °C = constant is reached, this rate of change drops to zero, which means that the cooling of the fuel pin is no longer increased. In addition, a part of the heat generated in this phase is used for fuel melting and thus removed from heat transfer.

When the gap has closed, a mechanical interaction between the fuel and the cladding begins as a consequence of the different rates of expansion. During this interaction, the stress on the cladding due to inner pressure becomes so high as to start plastic straining of the cladding. It is seen that the onset of plastic deformation largely depends on the original porosity of the fuel which, together with the volume of the gap, partly compensates the increase in volume during the change of phase of the fuel. After reduction of the melting rate the increased fuel expansion is partly maintained because the thermal coefficient of expansion of the melt is approximately twice that of solid fuel.

After this interpretation of the process of deformation we shall discuss a safety aspect. If, within the framework of reactor dynamics, the behaviour of an individual pin is extrapolated to a corresponding annular zone of the reactor, the condition of the fuel pin at the time of failure is a representative initial condition for the hypothetical core disassembly phase in this zone. In a fuel-coolant interaction (FCI), which is then possible, some of the thermal energy of the fuel is converted into kinetic energy of the coolant as a result of violent evaporation of sodium, the effect of which represents a mechanical stress upon core internals and the reactor vessel. The magnitude of energy conversion in the fuel-sodium interaction largely depends on the ratio between the masses of fuel and sodium and upon the fuel fragmentation, hence, the fraction of fuel molten [7, 8].

If it is assumed in this study that 3 % of a plastic deformation of a cladding already represents a burst criterion equivalent to the model in the sense mentioned above, the model pins "a" and "b" were destroyed within the period of time considered (see Fig. 5). Accordingly, pin "b" with the smaller gap width failed at t_V = 0.31 sec (fraction of molten fuel v_L = 0.69) prior to the reference pin "a" (t_V = 0.33 sec, v_L = 0.77). The reason of this sequence is obvious from Fig. 5. As mentioned above, melting of the fuel in pin "b" occurs at a relatively late date. The additional fuel expansion during phase changes can be compensated for by the smaller gap volume only for a moment and is transferred to the cladding at a comparatively earlier time. This causes excessive mechanical stress which is indicated by plastic deformation of the cladding.

With respect to the fuel-sodium interaction mentioned above, the smaller molten fraction in pin "b" as against "a" would cause a lower energy conversion. If one assumes that some of the fuel is expelled from the core area in the course of a fuel-sodium interaction [9], the nuclear excursion also would be slowed down earlier in this case, i. e., pin "b" in this study has the lower damage potential. In addition, as a consequence of the larger difference between the steady-state fuel temperature profile and the melting isotherms, this fuel pin also has a higher shutdown reserve due to the Doppler effect. Because of the comparatively high steady-state fuel temperatures this effect is felt least with pin "c". However, because of the relatively large porosity of the fuel, which represents a corresponding compensation capability with respect to the increase in volume associated with melting, it will sustain transient loads for the longest period of time.

Let me finally mention a comparison with data obtained by experiments. ANL evaluations of the transient tests of the S-series carried out in the TREAT reactor indicated that fuel pin failure occurred during the power impulse at an energy introduced into the fuel of 1800 .... 2000 J/g UO_2 [8].

The corresponding power integral for the reference pin "a" is approximately 1200 J/g UO_2. If one takes into account that in this case the excursion did not start from isothermal initial conditions (S3, S4, S5-tests: approximately 170 ^{o} C) but at steady-state operating temperatures, and if one adds the respective difference in enthalpy, this results in an amount of energy which is slightly above 1700 J/g UO_2. Taking into account a range of variation to the failure criterion and the different types of excursions, the computed results appear to be a realtistic approximation.

References

[1] Kuczera, B.: "BREDA - Ein Rechenmodell für die Verformung des Brennstabes eines Na-gekühlten Schnellen Brutreaktors unter transienter Belastung"
KFK 1729, Dec. 1972

[2] Kuczera, B.: "Die Verformung des Brennstabes eines Na-gekühlten Schnellen Brutreaktors unter transienter Belastung"
Paper HD-235, Reaktortagung des Deutschen Atomforums / KTG, Karlsruhe, April 1973

[3] Struwe, D.: "A two-dimensional Model for Fast Reactor Kinetics Analysis with Space Dependent Feedback"
Specialist Meeting on Reactivity Effects in Large Power Reactors (III.2), Ispra, Oct. 1970

[4] Keßler, G.: "Space-Dependent Dynamic Behaviour of Fast Reactors Using the Time-Discontinuous Synthesis Method"
Nucl. Sci. Eng. 41, 115 (1970)

[5] Kummerer, K.: Brennstäbe der Schnellbrüter-Prototypreaktoren"
Atomwirtschaft, Nov. 1972, p. 574

[6] Agrawal, A. K.: "Analysis of Fuel Meltdown Experiment (S-3) with the Transient Reactor Test (TREAT) Facility"
ANL-7610, Jan. 1970, p. 301

[7] Caldarola, L.: "A Theoretical Model for the Molten Fuel-Sodium Interaction in a Nuclear Fast Reactor"
Nucl. Eng. Design 22 (1972) 175 - 211

[8] Ivins, R. O., Wright, R. W.: "Fuel-Coolant Interactions"
ANL-7800, July 1971, p. 321

[9] Kastenberg, W. E., Rumble, E. T.: "Preliminary Analysis of the Predisassembly Phase of the Unprotected Overpower Transient Accident for SNR 300"
KFK 1782, Feb. 1973

a) Equations of Equilibrium

$$\frac{\partial \sigma_r}{\partial r} + \frac{\sigma_r - \sigma_\varphi}{r} = 0 \qquad \frac{\partial \sigma_z}{\partial z} = 0$$

b) Strain-Displacement Relations

$$\varepsilon_r = \frac{\partial u}{\partial r} \qquad \varepsilon_\varphi = \frac{u}{r}$$

$$\varepsilon_z = \frac{\partial w}{\partial z} = A = \text{const}$$

c) Hooke's Law (Deformation)

$$\varepsilon_r = \frac{1}{E}\left[\sigma_r - \nu\,(\sigma_\varphi + \sigma_z)\right] + \alpha T$$

$$\varepsilon_\varphi = \frac{1}{E}\left[\sigma_\varphi - \nu\,(\sigma_r + \sigma_z)\right] + \alpha T$$

$$\varepsilon_z = \frac{1}{E}\left[\sigma_z - \nu\,(\sigma_r + \sigma_\varphi)\right] + \alpha T$$

General Solution for the Fuel Cylinder
(Radial and Axial Displacement)

$$u(r) = \frac{1+\nu_B}{1-\nu_B} \cdot \frac{1}{r} \int_{R_1}^{r} \alpha_B(T) \cdot \eta \cdot T(\eta)\, d\eta + C_1 \cdot r + \frac{C_2}{r}$$

$$w(z) = Az + A_1$$

Fig. 1 Formulation of the Problem

(Cylindrical Coordinates)

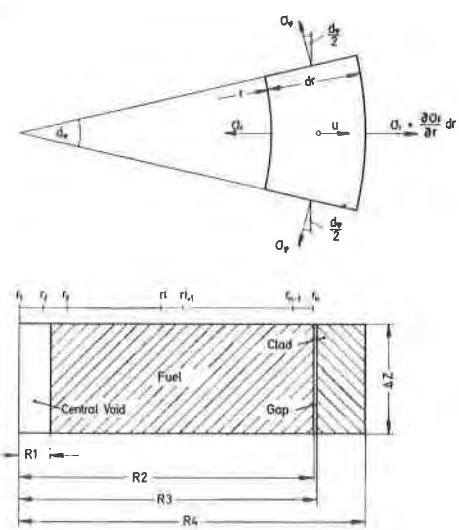

Fig. 2 Geometrie of the Fuel Pin (Axial Segment) and Stress Components

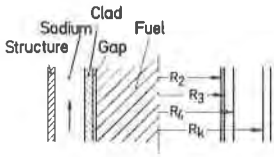

Single Fuel Pin Arrangement

Data of the Fuel Pin (a)

Pellet OR	R_2 = 2.55 mm [b: 2.57]
Cladding IR	R_3 = 2.62 mm
Cladding OR	R_4 = 3.00 mm
Equiv. Radius of Coolant Channel	R_k = 4.27 mm
Fuel	Mixed Oxide
Enrichment (PuO_2)	a = 0.21
Porosity	p = 0.07 [c: 0,12]
Volume change on fuel melting	Δv = 9%
Burnup	A = 0
Rod Power	X_0 = 420 W/cm
Power Excursion	$X(t) = X_0 (1+100 \cdot t)$
Coolant Inlet Temperature	T_{K1} = 380°C
Coolant Velocity	W_{Na} = 5.25 m/sec
Sectioning	10 ax. Segments
	10 rad. Regions of Fuel
	2 rad. Regions of Clad

Fig. 3 Arrangement and Data of the Fuel Pin

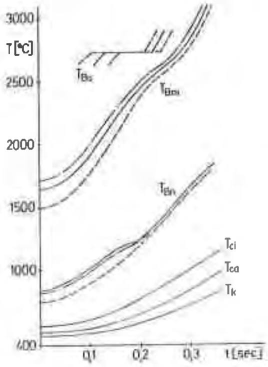

Fig. 4

Fuel Pin and Coolant Temperature as a Function of Time

T_{Bo} - Centerline Temperature
T_{Bm} - Average Temp. of Fuel
T_{Bn} - Fuel Surface Temp.
T_{ci} - Inner Clad Temp.
T_{ca} - Outer Clad Temp.
T_k - Coolant Temp.

——— Reference Pin „a"
– – – Pin „b" s = 0,05 mm
-·-·- Pin „c" Por = 0,12

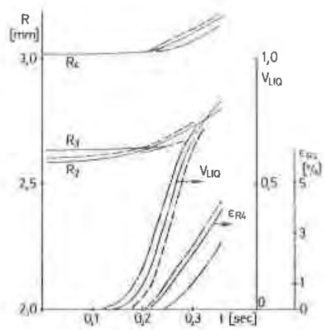

Fig 5

Dimensional Changes (R_2, R_3, R_4), Fraction of Molten Fuel (V_{LIQ}) and Plastic Deformation of the Clad (ε_{R4})